

Improving Radiologist Objectivity in The Detection of Transition Zone Prostate Cancer with Multi-Parametric 3.0T MRI

Patricia R. Castillo¹, Bryce K. Young^{1*}, Sannoh Punnen¹, Radka Stoyanova², Merce Jorda³, Vahara Tammisetti⁴, Felipe Munera¹

¹Department of Radiology, University of Miami/Jackson Health System, Miami, FL, U.S.A

²Department of Radiation Oncology, University of Miami, Miami, FL, U.S.A

³Department of Pathology, University of Miami, Miami FL, U.S.A

⁴Department of Radiology, University of Texas Health Science Center at Houston, Houston, TX, USA

***Corresponding author:** Bryce K. Young, Department of Radiology, University of Miami/Jackson Health System, Miami, FL, 1611 Northwest 12th Avenue, West Wing #279, Miami, FL 33136 U.S.A. Tel: (309) 453-3578; Email: brycekyoung@gmail.com

Citation: Castillo PR, Punnen S, Stoyanova R, Jorda M, Tammisetti V, et al. (2018) Improving Radiologist Objectivity in The Detection of Transition Zone Prostate Cancer with Multi-Parametric 3.0T MRI. ARCH URO REN DISEASES: RD-URO-10002.

Received Date: 04 September 2018; **Accepted Date:** 16 October 2018; **Published Date:** 24 October 2018.

Introduction

Prostate cancer is the second leading cause of cancer in American men with 161,360 cases resulting in 26,730 deaths in 2017 [1]. The prostate is divided in four anatomic zones; the peripheral zone, transition zone, central zone and the anterior stromal region, which contain approximately 80%, 20%, 5% and 0% of glandular tissue, respectively. While most of the prostate cancer occurs in the peripheral zone of the gland, approximately 20% of cancer arises within the transition zone [2,3]. Transition zone prostate cancer tends to have a larger tumor volume when compared to cancer occurring in the peripheral zone, albeit with a more favorable prognosis and better recurrence free survival [4-7].

The diagnostic performance of Magnetic Resonance (MR) Imaging in the evaluation of cancer occurring in the transition zone of the prostate has been less extensively studied than cancer occurring in the peripheral zone. On T2-weighted MR sequences, transition zone prostate cancer has characteristically been described as hypointense with an ill-defined shape, lenticular margins and lack of a capsule [8]. However, benign prostatic hyperplasia, which also occurs in the gland's transition zone, may mimic the appearance of prostate cancer on T2-weighted sequences [9-11]. In addition, prostatitis and fibrosis within the transition zone can also mimic prostate cancer on T2-weighted sequences, further interfering with the detection of prostate cancer [12].

The increased cellular density of prostate cancer results in restriction on Diffusion-Weighted Imaging (DWI), allowing for improved detection of prostate cancer [13]. DWI has been studied in the evaluation of transition zone prostate cancer with variable results. DWI utilizing b-values of < 1,000 sec/mm² have not been shown to significantly improve detection of transition zone

prostate cancer compared to T2-weighted MR imaging [14-16]. However, DWI using a b-value of 1,000 sec/mm² has been shown to improve detection of transition zone prostate cancer when compared to T2-weighted MR imaging [17,18]. Similarly, DWI utilizing ultra-high b-values of 2000 sec/mm² has shown to improve detection of transition zone prostate cancer when compared to b-values of 1,000 s/mm² [19-21]. Yet studies have demonstrated that there is no significant improvement of DWI using a b-value of 2,000 s/mm² over a b-value of 1,000s/mm² compared to T2-sequences [22-23]. Meanwhile, studies have demonstrated that a b-value of 1,500 s/mm² improves cancer detection compared to b-values of both 1,000 s/mm² and 2,000 s/mm² [20,24]. In addition, as b-values are increased, examinations can become limited due to loss of Signal to Noise Ratio (SNR) as well as susceptibility artifact [25,26]. Thus, a standardized b-value is therefore needed to optimize balance between image quality and detection of cancer in the transition zone of the prostate.

Apparent Diffusion Coefficient (ADC) sequences reconstructed from DWI have been used to assess cancer occurring in the transition zone of the prostate. It has been shown that cancerous lesions demonstrate lower absolute ADC values than non-cancerous lesions in the transition zone of the prostate [27-30]. Watanabe et. al. [27] and Sato et al. [28] reported mean ADC values of 1.01 x 10⁻³ s/mm² and 1.13 x 10⁻³ s/mm², respectively, for cancer occurring in the transition zone. Few studies have reported an optimal ADC cut-off value that could potentially be used to objectively discriminate benign from malignant lesions in the prostate. Nagayama et. al [29] determined an overall ADC cut-off value of 1.35 x 10⁻³ s/mm² for cancer occurring in the peripheral and transition zones, collectively. Wang. et. al [24] reported an ADC cut-off values of 0.77-0.92 x 10⁻³ s/mm² for cancer occurring in the transition zone. However, the results of these studies vary depending on the b-value chosen, the strength of the magnet, the coil type and imaging technique used. Thus, further studies demonstrating a more consistent absolute ADC value are needed that could potentially allow for the detection of cancer occurring in the transition zone of the prostate.

Dynamic contrast-enhanced imaging has also been studied in the evaluation of transition zone prostate cancer. However, studies have demonstrated suboptimal results as the vascularity of BPH can enhance like prostate cancer [18,31,32].

The aim of our current study is to retrospectively analyze a large patient cohort sample to comprehensively evaluate the performance of T2, ADC and dynamic contrast-enhanced sequences in the diagnosis of transitional zone prostate cancer. To optimize the balance between image quality and diagnostic accuracy we have chosen a b-value of 1,400 s/mm², which, to our knowledge, is the first study to evaluate this b-value. In addition, we hope to determine T2 and ADC values that can aid in the detection of transition zone prostate cancer.

1. Materials and Methods

1.1. Patient population

This retrospective single institution Health Insurance Portability and Accountability Act study was approved by our institutional review board and written informed consent was waived. Patients who had elevated prostate specific antigen levels were referred for MRI imaging of the prostate followed by Transrectal Ultrasound (TRUS) guided fusion biopsies between June 2014 and December 2015. The patient's electronic medical records were reviewed by the interpreting radiologists following image analysis. The mean patient age was 66.8 years (range

45-87 years) and the mean PSA level was 9.4 ng/ml (range 1.9-42.5 ng/ml). A total of 174 consecutive patients who had undergone biopsies of suspicious transition zone lesions were initially evaluated for inclusion in this study. Three patients were excluded due to suboptimal ADC maps secondary to susceptibility and motion artifacts, thus a total of 171 patients were included in this study. None of the patients had received prior radiation, chemotherapy, hormonal therapy or surgical intervention of the prostate.

1.2. MRI Imaging Technique

All examinations were performed on a 3.0 T MR scanner (Trio and Skyra, Siemens Healthineers, Erlangen, Germany or Discovery, General Electric, Milwaukee, Wisconsin). The patients were imaged in the supine position with a phased-array body coil placed over the pelvis. An endorectal coil was not utilized. The standard prostate MRI protocol used at our institution includes single shot turbo/fast spin echo T2-weighted axial and coronal localizer images through the pelvis (TR of 1000ms and TE of 87ms, slice thickness of 8mm, field of view (FOV) of 380 mm and matrix 256x256); turbo/fast spin echo T2-weighted axial, coronal and sagittal small field of view images without fat saturation through the prostate and seminal vesicles (TR of 3600ms and TE of 89ms, slice thickness of 3.0mm, FOV of 250mm and matrix of 256 x 320); turbo/fast spin echo T2-weighted axial images with fat-saturation through the pelvis (TR of 6100ms and TE of 114ms, slice thickness of 2.5mm, FOV of 380mm and Matrix 256x256); Echo planar axial DWI images through the prostate (TR of 7300 and TE of 112ms, slice thickness of 2.5mm, FOV of 380mm and matrix of 160x160 with b-values of 50s/mm², 500s/mm², 1,000s/mm² and 1,400s/mm²) and gradient-echo T1-weighted axial images without fat-saturation through the pelvis (TR of 5.08ms and TE of 2.3ms, slice thickness of 2.5mm, Field Of View (FOV) of 380mm and matrix 320x320). Dynamic contrast-enhanced axial T1 images without fat-saturation are obtained through the pelvis (TR of 4.3ms and TE of 1.9ms, slice thickness of 2.5mm, FOV of 250mm and matrix of 160x160) after injecting 0.1mm/kg of Multi-hance at 2.0cc per second followed by a 20ml saline flush. Dynamic contrast-enhanced images are obtained every 9.4 seconds for five minutes following injection of contrast.

1.2.1. Image Analysis

All MR images were reviewed on a picture archiving and communication system (PACS; IntelliSpace, Phillips Medical Systems, Best, Netherlands). Two radiologists, an abdominal imaging attending and abdominal imaging fellow, with eleven and two years of experience reading prostate MRI, respectively, analyzed the images in consensus. The radiologists were blinded to the histological results and the clinical findings of the patient. For the purposes of this evaluation, the transition zone was divided into the apical gland, mid gland and basal gland as well as into right and left halves using a sagittal plane through the verumontanum. The radiologists assigned a score on a five-point scale to transition zone lesions based upon their suspicion the lesion was cancerous as follows: 1-benign, 2-likely benign, 3-intermediate, 4-likely malignant and 5-definitely malignant. The T2-weighted sequences were analyzed first with prostate cancer defined as focus of hypo intensity with an ill-defined shape, lenticular margins, lack of a capsule and invasion of the anterior fibromuscular stroma [8]. The DW images and reconstructed ADC maps were subsequently analyzed with prostate cancer defined as a hyperintense focus on the DW images and a corresponding hypointense focus on the ADC maps. If two or more suspicious foci were identified within the transition zone, they were

scored individually. Regions of Interest (ROIs) were obtained of the suspicious lesions on the T2-weighted and ADC images, encircling approximately 80% of the lesion.

1.3. Histological

Biopsy specimens served as the reference standard. Each core biopsy is processed with four histological sections obtained from each core at 3-4 microns each. Slides #1 and #3 are stained with hematoxylin and eosin and #2 and #4 are kept unstained for immunohistochemical analysis if necessary. Histological evaluation is performed using the recommendations of the international society of urologic pathologists based of Gleason score and grade group [29].

1.4. Statistical

Receiver Operating Characteristic Curves (ROCs) and areas under the receiver operating characteristic curves (AUCs) were used to evaluate the accuracy of the T2-weighted and DWI sequences for the detection of transition zone prostate cancer. The ROCs were also used to determine an optimal cut-off value to differentiate cancerous and non-cancerous lesions on the ADC images. The sensitivity and specificity of the individual and combined T2 and DW sequences for detecting transition zone prostate cancer were obtained. In addition, the mean absolute T2 and ADC values were obtained for cancerous as well as non-cancerous lesions based on the measured ROIs. To evaluate the differences in absolute T2 and ADC values between cancerous and non-cancerous lesions, the unpaired student's t-test was utilized. A p-value of <0.05 was statistically significant.

2. Results

A total of 197 suspicious transition zone lesions were evaluated demonstrating 48 cancerous (24%) and 149 non-cancerous (76%) lesions. One patient had two foci of cancer within the transition zone, while the remainder of the patients had a single focus of cancer in the transition zone. Evaluating the lesions with ADC and T2-weighted sequences in tandem was found to improve accuracy in detecting cancer compared to either sequence alone. The sensitivity and specificity of the T2-weighted images for detecting transition zone cancer was 86% and 24%, respectively (Table 1). The sensitivity and specificity of the ADC images for detecting transition zone prostate cancer was 84% and 65%, respectively (Table 1). The sensitivity and specificity for detecting transition zone prostate cancer utilizing T2 and ADC imaging in tandem was 89% and 77%, respectively (Table 1). The sensitivity and specificity for dynamic contrast-enhanced sequences were 50% and 44%., respectively (Table 1). The AUCs for cancerous lesions were 0.84 on the T2-weighted sequences, 0.77 on the ADC sequences, and increased to 0.89 when analyzing the T2 and ADC sequences were analyzed together (Figures 1-3). The dynamic contrast-enhanced sequences demonstrated an AUC of 0.52 (Figure 5).

	Sensitivity	Specificity
T2	86%	24%
ADC	84%	65%

T2+ADC	89%	77%
DCE	50%	44%

Table 1: Sensitivity and specificity of T2, ADC, combined T2+ADC and dynamic contrast-enhanced sequences in the detection of transition zone prostate cancer.

Figure 1,2:

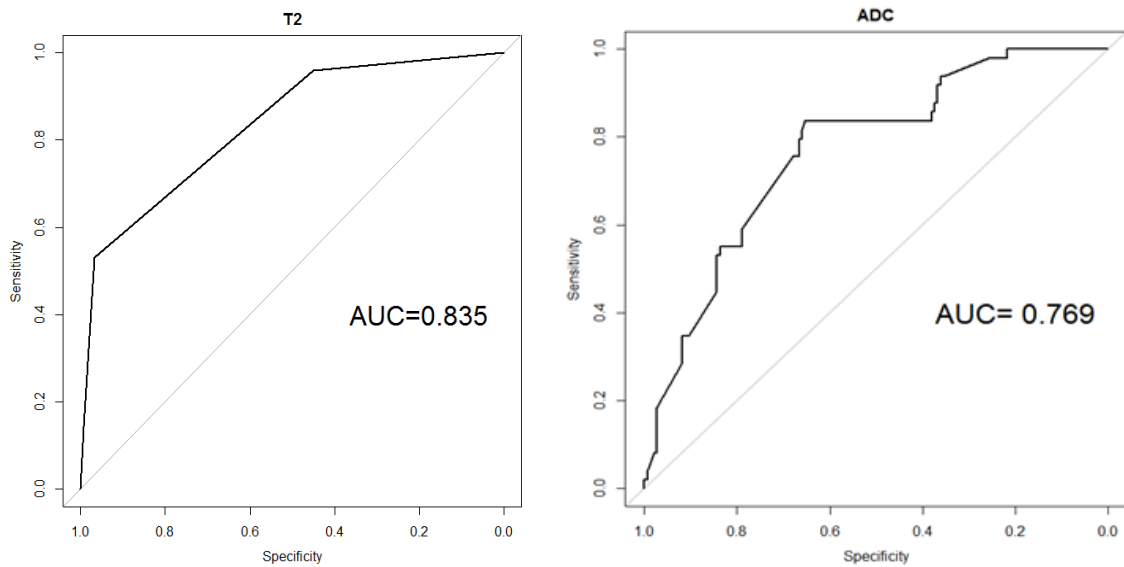
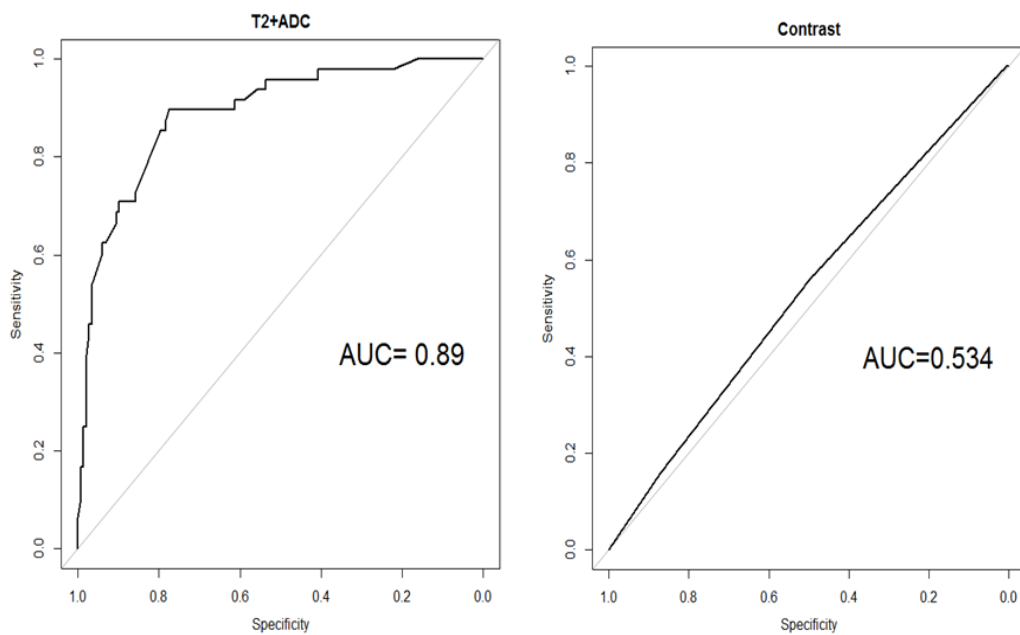


Figure 3,4:



Figures 1-4: Receiver Operator Characteristic (ROC) curves for T2, ADC, combined T2+ADC and dynamic contrast-enhanced sequences in the detection of transition zone prostate cancer. The AUCs for the T2 and ADC sequences individually were 0.84 and 0.77, respectively which increased to 0.89 when the sequences were evaluated in tandem. The dynamic contrast-enhanced sequences demonstrated an AUC of 0.53.

Figure 5:

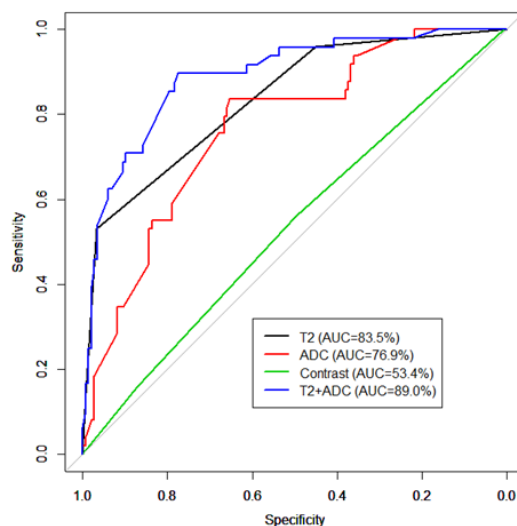


Figure 5: Combined Receiver Operator Characteristic (ROC) curves for T2, ADC, combined T2+ADC and contrast- enhanced sequences.

The mean absolute T2 and ADC values were found to be lower in cancerous lesions compared to non-cancerous lesions within the transition zone, although the differences were only statistically significant on the ADC images. The mean T2 value was 2.4 in cancerous lesions and 2.7 in non-cancerous lesions with standard deviations of 0.98 and 0.81, respectively ($p=0.29$) (Table 2). The mean ADC value was $0.73 \times 10^{-3} \text{ s/mm}^2$ for cancerous lesions and $0.92 \times 10^{-3} \text{ s/mm}^2$ for non-cancerous lesions ($p<.0001$) with standard deviations of $0.16 \times 10^{-3} \text{ s/mm}^2$ and $0.20 \times 10^{-3} \text{ s/mm}^2$, respectively (Table 2). The optimal cut-off value to differentiate cancer from non-cancerous lesions on the ADC sequences was determined to be $0.86 \times 10^{-3} \text{ s/mm}^2$, yielding a sensitivity of 84 % and specificity of 65% (Figure 6).

Figure 6:

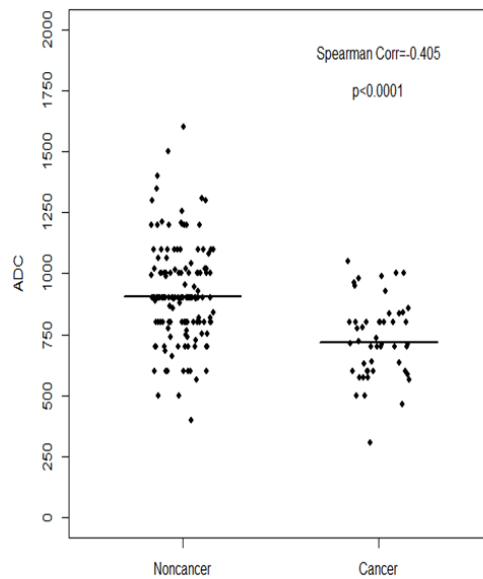


Figure 6: Scatter plot demonstrating ADC values for cancerous versus non-cancerous lesions in transition zone of the prostate. The mean ADC value was $0.73 \times 10^{-3} \text{ s/mm}^2$ for cancerous lesions and $0.92 \times 10^{-3} \text{ s/mm}^2$ for non-cancerous lesions ($p < .0001$) with standard deviations of $0.16 \times 10^{-3} \text{ s/mm}^2$ and $0.20 \times 10^{-3} \text{ s/mm}^2$, respectively.

	Mean T2 Value	Mean ADC Value
Cancer	2.4 +/- 0.98 s/mm ²	0.73 +/- 0.16 x 10 ⁻³ s/mm ²
Non-Cancer	2.7 +/- 0.81 s/mm ²	0.92 +/- 0.20 x 10 ⁻³ s/mm ²

Table 2: Mean T2 and ADC values for cancer and non-cancerous lesions in the transition zone of the prostate. The mean T2 and ADC values were both lower in cancerous lesions, compared to non-cancerous lesions. The differences were only statistically significant on the ADC sequences.

ADC value	Cut-off	Sensitivity	Specificity
-----------	---------	-------------	-------------

0.86 s/mm ²	x10 ⁻³	84%	65%
---------------------------	-------------------	-----	-----

Table 3: Optimal ADC cut-off value with corresponding sensitivity and specificity.

3. Discussion

The results of this study demonstrate that evaluating T2 and ADC sequences with a b-value of 1,400s/mm² in tandem is superior to evaluating either sequence alone in detecting transition zone prostate cancer. While this finding is comparable to prior studies evaluating b-values of 1000 s/mm² and 2,000 s/mm² [14-19], the diagnostic accuracy in our study with a b-value of 1,400s/mm² has outperformed prior studies. We found an AUC of 0.84 on the T2 sequences and an AUC of 0.77 on the ADC sequences, which increased to an AUC of 0.89 when the T2 and ADC sequences were evaluated in tandem. Jung et. al [18] reported an AUC of 0.60 on the T2 sequences, which increased to an AUC of 0.71-0.75 when the T2 and ADC sequences were analyzed in tandem with a b-value of 1,000s/mm². Katahira et. al [19] reported AUC of 0.65-0.72 on the T2 sequences, which increased to an AUC of 0.75-0.77 and when the T2 and ADC sequences were analyzed in tandem with a b-value of 1,000s/mm². The same study reported an increase in the AUCs to 0.82-0.85 when the T2 and ADC sequences were analyzed in tandem with a b-value of 2,000 s/mm².

It has been described that the diagnostic accuracy of detecting transition zone prostate cancer is limited on T2-sequences due to BPH [9-11]. On DWI, the increased cellular density of prostate cancer results in restricted diffusion, allowing for more accurate detection of cancer [13]. In our study, the T2 and ADC sequences have similar diagnostic accuracy and sensitivity, while the specificity of the ADC sequences is significantly higher. Hence, the diagnostic accuracy of evaluating the T2 and ADC sequences in tandem improves cancer detection compared to either sequence alone. However, as the b-value of DWI is increased, the signal to noise ratio decreases and susceptibility artifact increases, reducing lesion conspicuity [25,26]. We believe therefore diagnostic accuracy in our study with a b-value of 1,400 s/mm² has outperformed previous studies using b-values of up to 2,000s/mm². Therefore, evaluating T2 and DWI sequences in tandem with a b-value of 1,400 s/mm² may provide an optimal balance between diagnostic accuracy and image quality for the detection of transition zone prostate cancer. While prior studies have not evaluated a b-value of 1,400 s/mm², our findings are comparable with two prior studies that evaluated a slightly higher b-value of 1,500 s/mm² [20,24].

Furthermore, we have determined ADC values are lower in cancer compared to non-cancerous lesions in the transition zone of the prostate (Figures 7-10). The mean ADC value was 0.73 x 10⁻³ s/mm² for cancerous lesions and 0.92 x 10⁻³ s/mm² for non-cancerous lesions (p<.0001). An important result of this study is that we have determined that an ADC cut-off value of 0.86 x10⁻³ s/mm² with a sensitivity of 84% and a specificity of 77% is optimal to differentiate cancer from non-cancerous lesions in the transition zone of the prostate. This value provides an objective measure to accurately discriminate benign from malignant lesions, independent from other imaging sequences. The transition zone is often missed on random systematic biopsies. This ADC cut-off value could allow for the localization of transition zone prostate cancer for

targeted biopsy, potentially reducing false negative biopsy results. In addition, this value could be used for disease staging, treatment planning and monitoring response to treatment. While prior studies have demonstrated that cancerous lesions appear with lower ADC values than non-cancerous lesions, the results are often reported as mean values [27-30]. Few studies have determined an ADC cut-off value. Nagayama et. al [29] reported an overall mean ADC cut-off level of $1.35 \times 10^{-3} \text{ s/mm}^2$ with a sensitivity of 88% and a specificity of 96% for peripheral and transition zone cancer, collectively. Wang. et. al [24] reported ADC cut-off values of 0.77-0.92 with sensitivities of 69.4%-77.3% and specificities of 81.6-90.4% for cancer occurring in the transition zone. This is the first study to evaluate ADC values using b-values of 0 s/mm^2 and $1,400 \text{ s/mm}^2$, which we believe provides an optimal balance between diagnostic accuracy and image quality, accounting for our lower absolute ADC value and higher sensitivity.

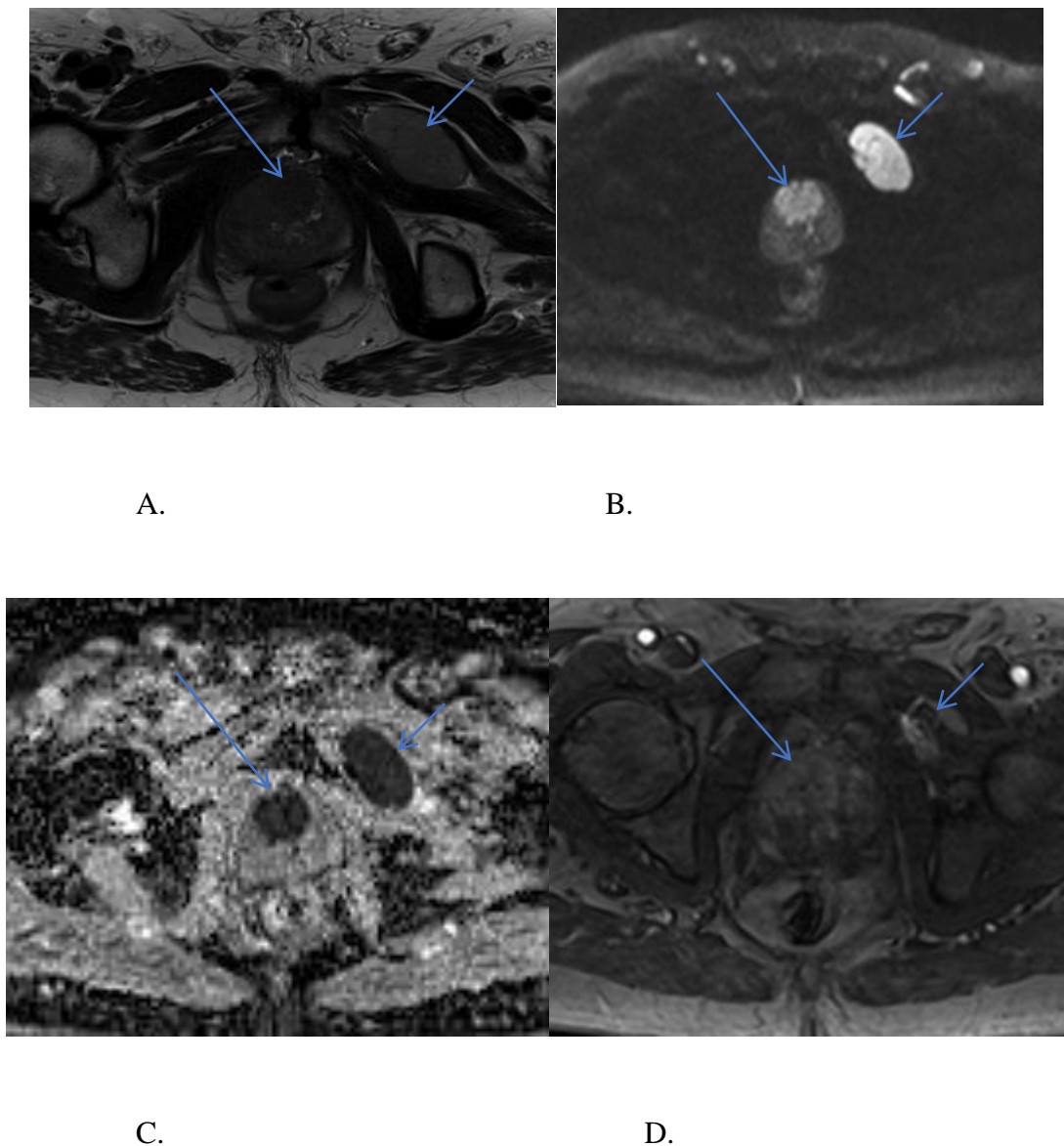
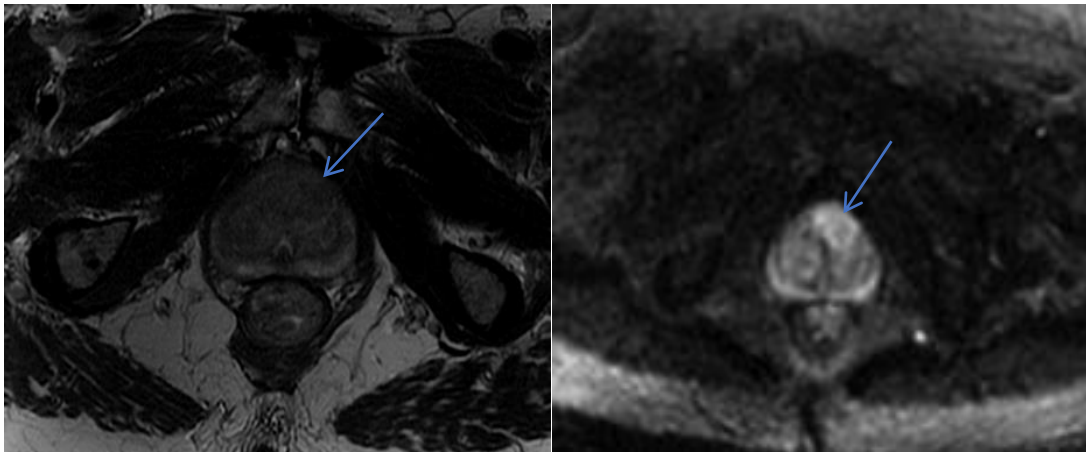


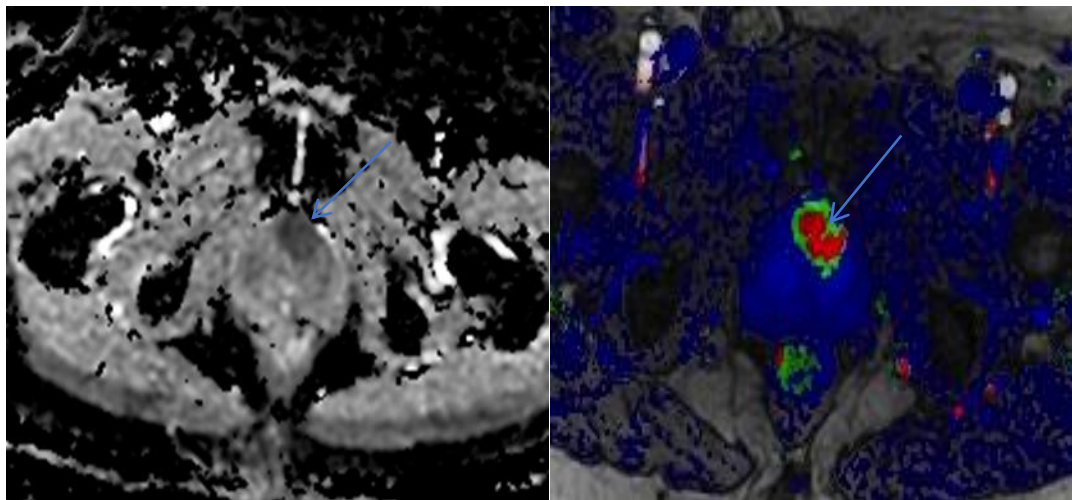
Figure 7 A-D: A. T2-weighted, Diffusion-weighted, Apparent Diffusion Coefficient and Dynamic contrast-enhanced images demonstrating a suspicious lesion in the transition zone of

the prostate (long arrow). The lesion is hypointense on T2 sequences (A), hyperintense on DWI sequences (B), hypointense on the ADC sequences (C) and demonstrates enhancement following the administration of contrast (D). The region of interest is placed centrally within the lesion on the ADC sequences(C) and measures $0.55 \times 10^{-3} \text{ s/mm}^2$, which is below the ADC cut-off value determined in this study of $0.86 \times 10^{-3} \text{ s/mm}^2$. The lesion was biopsy proven Gleason grade 5 transition zone prostate cancer. There is associated lymphadenopathy (short arrow).



A.

B.

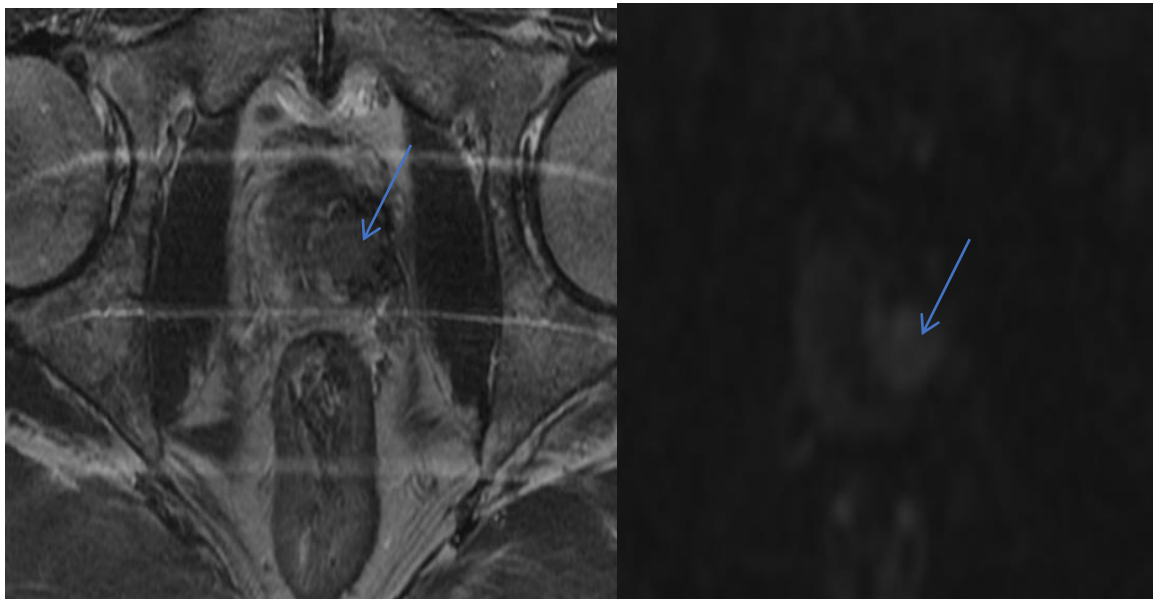


C.

D.

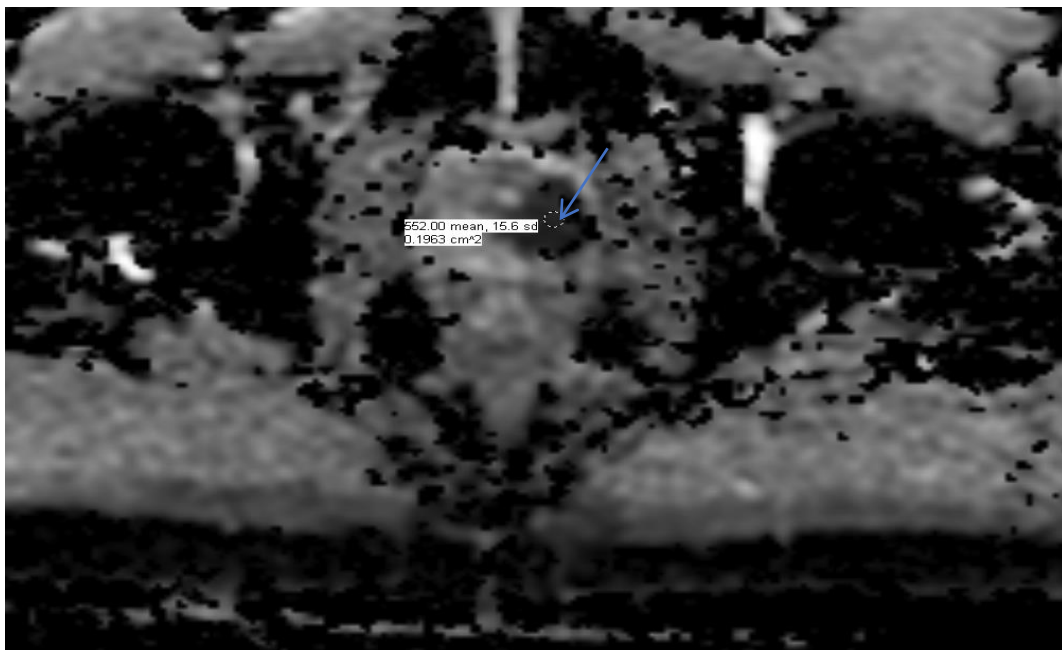
Figure 8: A-D: T2-weighted, Diffusion-weighted, Apparent Diffusion Coefficient and Dynamic Contrast enhanced images demonstrating a suspicious lesion in the transition zone of the prostate (arrow). The lesion is hypointense on T2 sequences (A), hyperintense on DWI sequences (B), hypointense on the ADC sequences (C) and demonstrates enhancement

following the administration of contrast (D). This lesion was biopsy proven Gleason Grade 4 transition zone prostate cancer.



A.

B.



C.

Figure 9: A-C: T2-weighted, Diffusion-weighted, and Apparent Diffusion Coefficient images demonstrating a suspicious lesion in the transition zone of the prostate (arrow). The lesion is hypointense on T2 sequences (A), hyperintense on DWI sequences (B) and hypointense on the ADC sequences (C). The region of interest is placed centrally within the lesion on the ADC sequences in figure C and measures $0.55 \times 10^{-3} \text{ s/mm}^2$, which is below the ADC cut-off value determined in this study of $0.86 \times 10^{-3} \text{ s/mm}^2$. This lesion was biopsy proven Gleason Grade 3 transition zone prostate cancer.

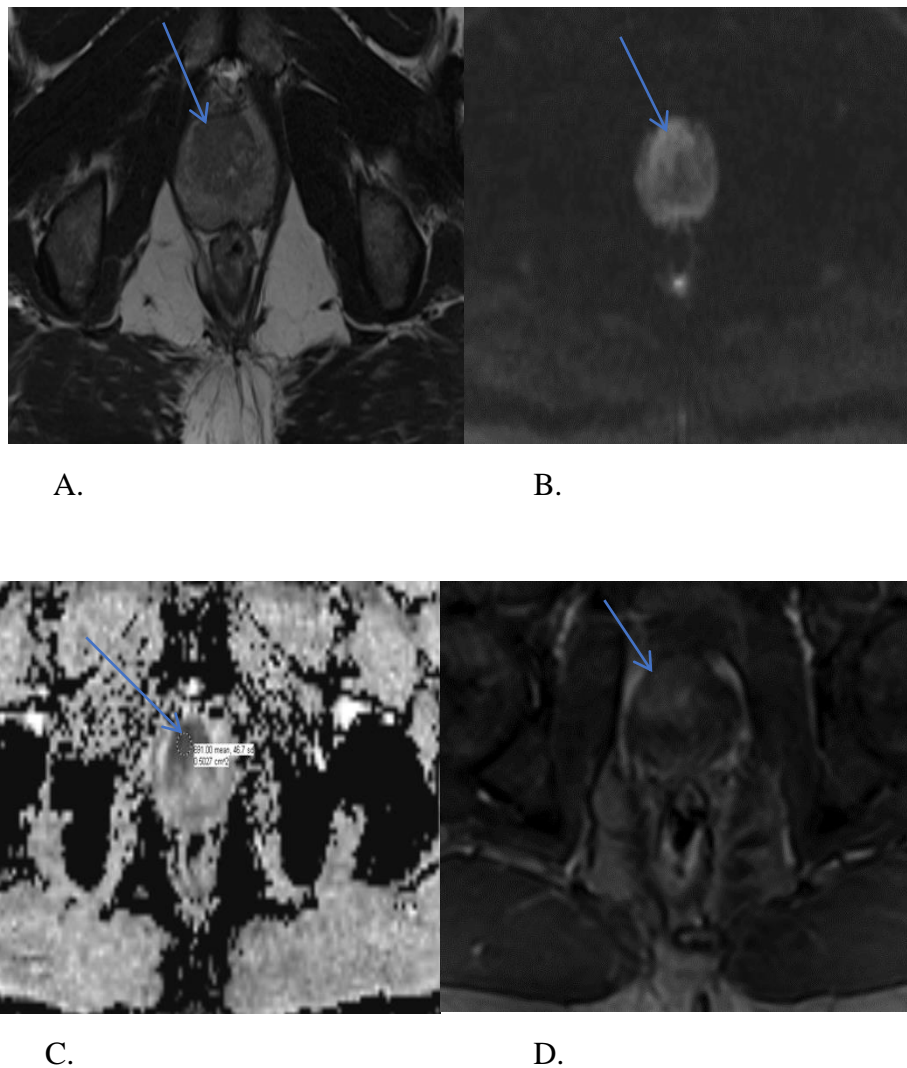


Figure 10: A-D: T2-weighted, Diffusion-weighted, Apparent Diffusion Coefficient and Dynamic Contrast enhanced images demonstrating a suspicious lesion in the transition zone of the prostate (arrow). The lesion is hypointense on T2 sequences (A), hyperintense on DWI sequences (B), hypointense on the ADC sequences (C) and demonstrates enhancement following the administration of contrast (D). The region of interest is placed centrally within the lesion on the ADC sequences (C) and measures $0.69 \times 10^{-3} \text{ s/mm}^2$, which is below the ADC cut-off value determined in this study of $0.86 \times 10^{-3} \text{ s/mm}^2$. This lesion was not proven to be cancer following biopsy and represents a false positive.

The results of our study also demonstrate that absolute T2 values are lower in cancerous lesions when compared to non-cancerous lesions, although the differences were not statistically significant. The mean T2 value was 2.4 in cancerous lesions and 2.7 in non-cancerous lesions ($p=0.29$). The lack of statistical significance is likely due to the similar T2-signal hypo intensity of prostate cancer to benign conditions including BPH and fibrosis [8]. Moreover, the dynamic contrast-enhanced sequences were not found to be helpful in the detection of transition zone prostate cancer. These results are concordant with prior studies [18,31,32] and are thought to be attributable to the increased vascularity of BPH, which can enhance like prostate cancer.

This study had several limitations. The radiologists were specifically looking for transition zone cancer, which may have introduced selection bias. The radiologists evaluated the T2, DW and ADC sequences sequentially which may have also introduced selection bias. Given the small size of the lesions, it is possible benign prostate tissue may have been included in the ROI measurements, resulting in measurement bias. In addition, although targeted biopsies of the lesions were performed, it is possible sampling error may have occurred. One false positive result was encountered in this study (Figure 10), which is thought to be due to sampling error. Correlation of biopsy tissue with prostatectomy specimens could be helpful for further evaluation. Furthermore, although we evaluated a b-value of $1,400\text{s/mm}^2$, additional b-values were not evaluated for comparison. Future studies evaluating a spectrum of b-values would be beneficial. Lastly, this study was retrospective, and a prospective study is warranted.

In conclusion, this is a large, comprehensive study that demonstrates that evaluating T2 and ADC sequences in tandem is superior to evaluating either sequence alone in the detection of transition zone prostate cancer, while dynamic contrast-enhanced sequences were not found to be helpful. We have also shown that cancerous lesions demonstrate lower absolute ADC values than non-cancerous lesions with an optimal cut-off value of $0.86 \times 10^{-3} \text{ s/mm}^2$. These results could potentially aid in transition zone prostate detection, biopsy targeting, treatment planning and disease surveillance. This was the first study to obtain these results with a b-value of $1,400 \text{ s/mm}^2$, which we believe provides an optimal balance between image quality and diagnostic accuracy.

References

1. <http://www.cancer.org/cancer/prostatecancer/detailedguide/prostate-cancer-key-statistics>.
2. McNeal JE, Redwine EA, Freiha FS, Stamey TA (1988) Zonal distribution of prostatic adenocarcinoma: correlation with histologic pattern and direction of spread. *Am J Surg Pathol* 12: 897-906.
3. Reissigl A, Pointner J, Strasser H, Ennemoser O, Klocker H, et al. (1997) Frequency and clinical significance of transition zone cancer in prostate cancer screening. *Prostate*; 30:130-135.
4. Noguchi M, Stamey TA, Neal JE, Yemoto CE (2000) An analysis of 148 consecutive transition zone cancers: clinical and histological characteristics. *The Journal of urology* 163: 1751-1755.
5. Augustin H, Hammerer PG, Blonski J, Graefen M, Palisaar J, et al. (2003) Zonal location of prostate cancer: significance for disease-free survival after radical prostatectomy? *Urology* 62:79-85.
6. King CR, Ferrari M, Brooks JD (2009) Prognostic significance of prostate cancer originating from the transition zone. *Urologic oncology* 27: 592-597.
7. Lee JJ, Thomas I-C, Nolley R, Ferrari M, Brooks JD, et al. (2015) Biologic Differences Between Peripheral and Transition Zone Prostate Cancer. *The Prostate* 75: 183-190.
8. Akin O, Sala E, Moskowitz CS, Kuroiwa K, Ishill NM, et al. (2006) Transition zone prostate cancers: features, detection, localization, and staging at endorectal MR imaging. *Radiology* 239:784-792

9. Schiebler ML, Tomaszewski JE, Bezzi M, Pollack HM, Kressel HY, et al. (1989) Prostatic carcinoma and benign prostatic hyperplasia: correlation of high-resolution MR and histopathologic findings. *Radiology* 172: 131-137.
10. Grossfeld GD and Coakley FV (2000) Benign Prostatic hyperplasia: Clinical Overview and Value of Diagnostic Imaging. *Radiol Clin North Am* 38: 31-47.
11. Ikonen S, Kivisaari L, Tervahartiala P, Vehmas T, Taari K, et al. (2001) Prostatic MR imaging: Accuracy in differentiating cancer from other prostatic disorders. *Acta Radiol* 42: 348-354.
12. Lovett K, Rifkin MD, McCue PA, Choi H (1992) MR Imaging Characteristics of Noncancerous Lesions of the Prostate. *J Magn Reson Imaging* 2: 35-39.
13. Kayhan A, Fan X, Oommen J, Oto A (2010) Multi-parametric MR imaging of transition zone prostate cancer: Imaging features, detection and staging. *World J Radiol* 2: 180-187.
14. Delonchamps NB, Rouanne M, Flam T, Beuvon F, Liberatore M, et al. (2011) Multiparametric Magnetic Resonance Imaging for the detection and localization of prostate cancer: Combination of T2-weighted, Dynamic Contrast-Enhanced and Diffusion Weighted Imaging. *BJU Int* 107: 1411-1418.
15. Haider MA van der Kwast TH, Tanguay J, Evans AJ, Hashmi AT, et al. (2007) Combined T2-weighted and diffusion-weighted MRI for localization of prostate cancer. *AJR Am J Roentgenol* 189: 323-332.
16. Hoeks CMA, Hambroek T, Yakar D, Hulsbergen-van de Kaa CA, Feuth T, et al. (2013) Transition zone prostate cancer: detection and localization with 3-Tmultiparametric MR imaging. *Radiology* 266: 207-217.
17. Yoshizako T, Wada A, Hayashi T, Uchida K, Sumura M, et al. (2008) Usefulness of diffusion-weighted imaging and dynamic contrast-enhanced magnetic resonance imaging in the diagnosis of prostate transition-zone cancer. *Acta Radiol* 49: 1207-1213.
18. Jung SI, Donati OF, Vargas HA, Goldman D, Hricak H, et al. (2013) Transition zone prostate cancer: incremental value of diffusion-weighted endorectal MR imaging in tumor detection and assessment of aggressiveness. *Radiology* 269: 493-503.
19. Katahira K, Takahara T, Kwee TC, Oda S, Suzuki Y, et al. (2011) Ultra-high-b-value diffusion-weighted MR imaging for the detection of prostate cancer: evaluation in 201 cases with histopathological correlation. *Eur Radiol*;21(1):188-196.
20. Metens T, Miranda D, Absil J, Matos C (2012) What is the optimal b-value in diffusion-weighted MR imaging to depict prostate cancer at 3 T? *Eur Radiol*, 22: 703-709.
21. Tsutomu T, Kanomata N, Sone T, Yoshimasa Jo, Yoshiyuki Miyaji, et al. (2014) "High B Value (2,000 s/mm²) Diffusion-Weighted Magnetic Resonance Imaging in Prostate Cancer at 3 Tesla: Comparison with 1,000 s/mm² for Tumor Conspicuity and Discrimination of Aggressiveness.
22. Kitajima K, Takahashi S, Ueno Y, Yoshikawa T, Ohno Y, et al. (2012) Clinical utility of apparent diffusion coefficient values obtained using high b-value when diagnosing prostate cancer using 3 Tesla MRI: comparison between ultra-high b-value (2000 s/mm²) and standard high b-value (1000 s/mm²). *J Magn Reson Imaging*, 36: 198-205.
23. Kim CK, Park BK, Han JJ, Kang TW, Lee HM (2007) Diffusion-weighted imaging of the prostate at 3 T for differentiation of malignant and benign tissue in transition and peripheral zones: preliminary result. *J Comp Assist Tomogr* 31: 449-454.
24. Wang X, Qian Y, Liu B, Cao L, Fan Y, et al. (2010) High-b-value diffusion-weighted MRI for the detection of prostate cancer at 3T. *Clinical Radiology*; 69: 1165-1170.
25. Manenti G, Nezzo M, Chegai F, Vasili E, Bonanno E, et al. (2014) DWI of Prostate Cancer: Optimal b-Value in Clinical Practice. *Prostate Cancer* 2014.
26. Chan Kyo Kim, Byung Kwan Park, Bohyun Kim (2010) Diffusion-Weighted MRI at 3 T for the Evaluation of Prostate Cancer. *American Journal of Roentgenology*, 194: 1461-1469.
27. Watanabe Y, Nagayama M, Araki T, Terai A, Okumura A, et al. (2013) Targeted biopsy based on ADC map in the detection and localization of prostate cancer: A feasibility study. *J. Magn. Reson. Imaging* 37: 1168-1177.
28. Sato C, Naganawa S, Nakamura T, Kumada H, Miura S, et al. (2005) Differentiation of noncancerous tissue and cancer lesions by apparent diffusion coefficient values in transition and peripheral zones of the prostate. *J. Magn. Reson. Imaging* 21: 258-262.
29. Nagayama M, Watanabe Y, Terai A, Araki T, Notohara K, et al. (2011) Determination of the cutoff level of apparent diffusion coefficient values for detection of prostate cancer. *Jpn J Radiol* 29: 488
30. Tamada T, Sone T, Jo Y, Toshimitsu S, Yamashita T, et al. (2008) Apparent diffusion coefficient values in peripheral and transition zones of the prostate: Comparison between normal and malignant prostatic tissues and correlation with histologic grade. *J. Magn. Reson. Imaging* 28: 720-726.
31. Oto A, Kayhan A, Jiang Y, Tretiakova M, Yang C, et al. (2010) Prostate cancer: Differentiation of Central Gland Cancer from Benign Prostatic Hyperplasia by Using Diffusion-Weighted and Dynamic Contrast-Enhanced MR Imaging. *Radiology* 257: 715-723.

32. Van Niekerk, Witjes CG, Barentsz JA, van der Laak JO, JAWM, et al. (2013) Microvasculature in Transition Zone Prostate Tumors Resembles Normal Prostatic Tissue. *Prostate* 73: 467-475.
33. *Acta Pathologica, Microbiologica, et Immunologica Scandinavica* 2016. 124: 433-435.